Overview of the ANITA project

Steven Barwick[b], James Beatty[c], David Besson[d], John Clem[e], Stephane Coutu[c], Michael DuVernois[f], Paul Evenson[e], Peter Gorham[*g], Francis Halzen[h], Abram Jacobson[i], David Kieda[j], John Learned[g], Kurt M. Liewer[a**], Stephen Lowe[a], Charles Naudet[a], Allen Odian[k], David Saltzberg[l], David Seckel[e]

[a]Jet Propulsion Laboratory; [b]University of California, Irvine; [c]Pennsylvania State University; [d]University of Kansas; [e]University of Delaware; [f]University of Minnesota; [g]University of Hawaii at Manoa, [h]University of Wisconsin; [i]Los Alamos National Laboratory; [j]University of Utah; [k]Stanford Linear Accelerator; [l]University of California, Los Angeles

ABSTRACT

The ANITA project is designed to investigate ultra-high energy (>10^{17} eV) cosmic ray interactions throughout the universe by detecting the neutrinos created in those interactions. These high energy neutrinos are detectable through their interactions within the Antarctic ice sheet, which ANITA will use as a detector target that effectively converts the neutrino interactions to radio pulses. This paper will give an overview of the project including scientific objectives, detection description and mission design.

Keywords: ANITA, High energy neutrinos, Antarctica, balloon

1. SCIENTIFIC GOALS AND OBJECTIVES

The primary objectives of the Antarctic Impulsive Transient Antenna (ANITA) mission are to extend the reach of NASA observatories into the realm of high energy neutrino astronomy, and thereby to investigate and constrain the nature of the sources of the highest energy cosmic ray particles, by direct detection and characterization of the neutrinos that are predicted to be strongly correlated to them[1]. The observation over the last 40 years of several dozen cosmic ray events with single-particle energies of up to 50 Joules (equivalent to a major-league fastball) poses among the most intriguing and intractable problems in high-energy astrophysics. No known process can give rise to particles of energies a billion times higher than those produced in man-made accelerators, as these have. Stated simply, these particles should not exist. Yet in fact they do exist and continue to be observed with regularity every year. If they arise from sources at cosmological distances (for example, from unknown processes in gamma- ray bursts) then they should not be able to propagate to Earth without being utterly absorbed. Yet if they arise from sources near enough to avoid absorption, we are at a loss to identify their sources. Observations of high-energy neutrinos are one of the crucial keys to unlock this mystery. If, on the one hand, the

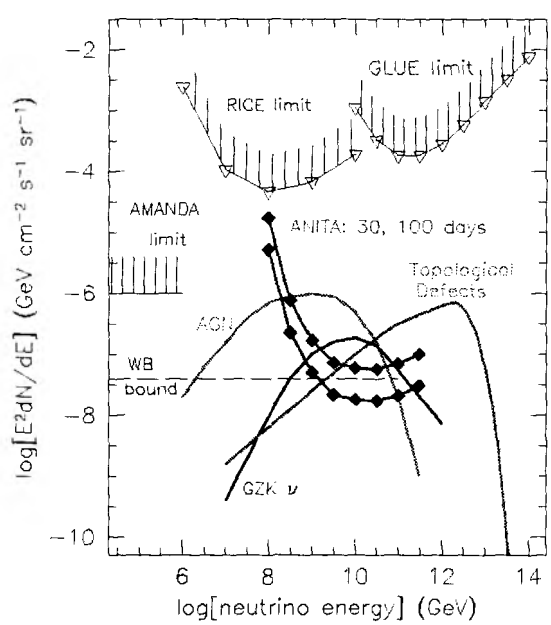

Figure 1: Various neutrino models and experiment limits are shown along with estimates of the ANITA sensitivity for two different flight times.

* Principal Investigator, gorham@phys.hawaii.edu, Univ. of Hawaii at Manoa, 2505 Correa Rd, Honolulu, HI, 96822
** Presenter, kurt.liewer@jpl.nasa.gov, Jet Propulsion Laboratory, 4800 Oak Grove Drive, CA, 91011, USA

sources are at cosmological distances, then there is a corresponding and closely coupled flux of neutrinos that result from the summed interactions of these cosmic rays throughout the universe. This process occurs at an absorption edge known as the Greisen-Zatsepin-Kuzmin (GZK) cut-off, postulated first in the early 1960's.[2,3] If, on the other hand, these particles arise from sources local to our galaxy or the Local Group of galaxies, then high-energy neutrinos are still the most likely and compelling signature of the potentially exotic processes in these local interactions.[4,5,6] Under almost any conceivable theory, the observation of associated high-energy neutrinos (or even significant limits to their flux) provides necessary and in many cases sufficient evidence to decide between the competing models. ANITA will provide the very first opportunity to view the landscape of the ultra-high energy universe, unaffected by absorption, for neutrinos propagate freely to Earth even from cosmological distances.

1.1. Historical background

Beginning in the early 1960's, when measurements using ground-based particle arrays first reported results showing that some of the events detected were at almost unbelievable energies in excess of several times 10^{19} eV [6], the evidence for the existence of single particles with Joule-scale energies has continued to grow. Compounding this mystery are several theoretical and experimental observations. First, work by K. Greisen[2], and simultaneously G. Zatsepin and V. Kuzmin[3] in the early 60's showed that the presence of the newly discovered microwave background radiation provides a severe constraint on the origin of such particles. This is due to the fact that, in the rest frame of a proton or nucleus at such energies, the 3K background radiation is boosted to gamma-ray energies by the Lorentz factor (~ 10^{11}) of the hadrons. Thus the cross section for interaction is high enough that the mean free path for a hadronic particle is of order 4 Mpc, only slightly larger than the Local Group of galaxies. This constraint implies that, if the sources of the highest energy particles are at average distances large compared to this absorption edge, or GZK cutoff as it is known, then the spectrum of the particles should fall off sharply beyond $5x10^{19}$ eV. The second observation, an experimental one, provides the real conundrum: no clear cutoff in particle energies has been observed to date in a variety of experiments [7]; yet no likely sources can be identified within the GZK volume at a radius of several times the mean interaction length. Compounding this problem is the fact that, while some preliminary evidence for inhomogeneity in the event source directions has been reported[8], none of the possible preferred directions point back to sources that are near enough to be considered candidates within the GZK horizon. In fact, because all known charge hadron acceleration processes also yield copious neutrino production (typically through pion decay), several of the more favored models for producing the super-GZK events include significant roles for neutrinos, either as messenger particles for sources at cosmological distances[9], or as secondaries which will carry the information about the primary particle fluxes.[10] Fig. 2 shows an example of the measured cosmic ray spectrum, the GZK cutoff, and estimates for the associated GZK neutrino fluxes. At the present time, the existing experimental measurements have established the existence of these particles through detection of only a few tens of events above 10^{20} eV. Because of the relatively small numbers of events, the overall integral flux of these particles is uncertain to at least a factor of 2. In the most recent results, reported at the 27th ICRC in Hamburg, the controversy over the nature of the spectrum around the GZK cutoff has increased, with some groups reporting increased evidence for super-GZK events which appear clustered on the sky[11], and others reporting results possibly still consistent with the GZK cutoff, and no super-GZK events.[12] The spectrum of neutrinos is uniquely sensitive to the exact nature of the process that gives rise to the GZK cutoff, or to scenarios in which it is violated. The observation of such neutrinos would have profound implications for the sources of such particles. At these energies, neutrinos are the only known particles that have the penetrating power to allow for imaging capability in the traditional

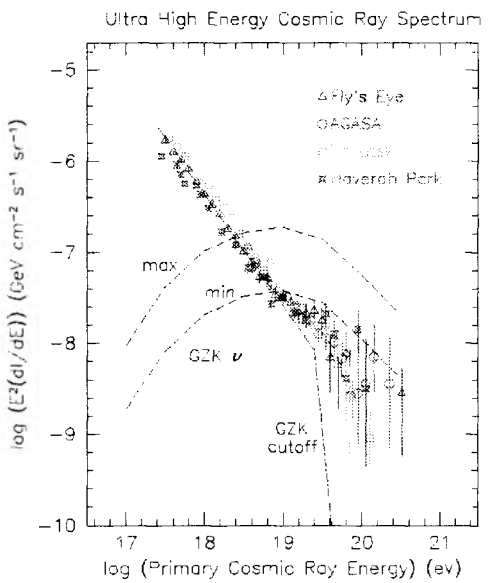

Figure 2: The world spectrum of EHE cosmic rays near the GZK cutoff energy, and estimates for GSK neutrinos.

sense of astronomy, for photons and charged hadrons suffer either absorption or magnetic deflection and thus lose information about their original source. Neutrinos are in fact the *only* known EeV particles that can reach us from cosmological distances. They can thus carry information about either the primary source directly, or about the global energy losses of the GZK particles, thus testing production and propagation scenarios for the super-GZK cosmic rays[13,1].

1.2. The neutrino detection problem

One of the great impediments to advances in detection of either the super-GZK cosmic rays or their possible neutrino counterparts is the extremely low flux density of these particles, of order 1 per km^2 per century above 10^{20} eV. To make noticeable progress on a 1 year timescale, a cosmic ray detector must have an area x solid angle product (here denoted as the aperture) of order several thousand km^2 x sr. For neutrino detection, the relevant measure of a detector is a water-equivalent volume x solid angle product, and at least several hundred km^2 x sr water equivalent is required. Another important necessity is high duty cycle, since it is ultimately the total exposure time of the detector volume that provides the event collection.

The problem is in some sense analogous to early observations of gamma-ray bursts, before there were adequate statistics to establish that the burst sources could not be galactic or halo sources. The real need in this case is similar: greater statistics on the actual events. At present the world sample of super-GZK events is of order several dozen, and grows only infinitesimally each year because of the rarity of the events collected by presently available apertures in ground-based installations. Although improvements in ground-based installations, and several new observatories are planned within the next decade, major advances in this problem will most likely require synoptic monitoring of a large area of the Earth's atmosphere from an orbital observatory, such as the proposed mission OWL and EUSO missions.

2. BASELINE MISSION OVERVIEW

ANITA will make use of radio emission from the secondary electromagnetic cascade induced by a neutrino interaction within the Antarctic ice sheet. Neutrino events anywhere within the million square kilometer area viewed by the instrument from the 37 km altitude of the balloon floating over the Antarctic ice sheet will be detected. The remarkable transparency of Antarctic ice to radio waves makes this experiment possible, and the enormous volume of ice that can be simultaneously monitored leads to an unparalleled sensitivity to neutrinos in the energy range of 0.1 to 100 EeV. ANITA will obtain a total of 30 days live-time as part of our baseline mission. A conservative approach has been adopted toward achieving the planned 30 day live-time, basing this total on 3 Antarctic flights, each of which achieves an average of 10 days of live-time. Clearly a more cost-effective approach will be to make use of multiple orbits around the pole if and when these become available to Antarctic balloon missions. During the flight, ANITA will maintain a nominal altitude of 37 km; however, loss of even up to 10 km of altitude would not constitute mission failure unless the balloon flight path did not remain over the ice sheet. The reason for this is that a lower altitude and the corresponding loss of viewed volume of ice is compensated for by increased sensitivity to lower energy neutrinos due to the reduced range.

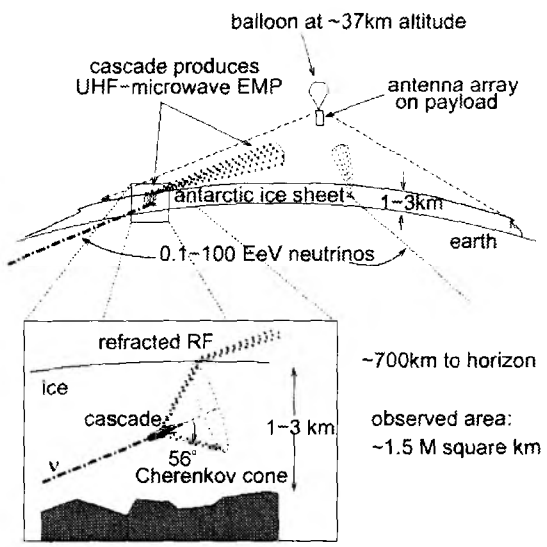

Figure 3: Schematic of the ANITA concept

Figure 3 shows the observation geometry.

2.1. Measurements and analysis

ANITA will provide measured geolocated positions, estimated energy, and derived track direction in celestial coordinates for a set of candidate neutrino-induced cascades above an energy of about $3x10^{17}$ eV. These will all be measured at modest resolution but with high sensitivity. The basic analysis approach will be to establish a matched-filter type of template for rejection of all spurious interference and

thermal noise triggers, based on models and instrument calibration data. ANITA is unusual for a NASA astrophysics mission because the expected numbers of detected events from neutrino EMP within the ice is far smaller than that due to background, and background rejection will be fundamental to all data analysis. We anticipate background rejection factors of order 10^4 based on our experience with other investigations. Background rejection factors 1-2 orders of magnitude higher are now routinely achieved in high energy physics experiments, upon which much of the ANITA hardware and trigger logic is based. If no candidate events are detected, we will provide careful estimates of the sensitivity which will be used to derive a firm upper limit to the flux density of the neutrinos in this energy regime. ANITA will thus act as a road-building mission to pave the way for more complex and precise neutrino observatories which can measure the neutrino spectrum with much better precision. ANITA is analogous to the early X-ray sounding rockets: it will give an early glimpse at the nature of the high energy neutrino spectrum, which affords a corresponding look at the nature of the sources of the highest energy cosmic rays.

2.2. Data products and science results

The raw data products produced by ANITA are the detected events themselves, sorted into quality groups according to the likelihood that they originate from a neutrino cascade. This raw data archive will form the basis for a processed set of neutrino candidates for which the science team will determine the best fit energy of the cascade, and the direction of the original neutrino that caused it. The precision to which this can be done will depend on several factors, which will be mentioned later in the instrument design section. The fundamental science objective of the detection of neutrinos associated with the GZK cosmic rays can be further refined into three aspects, basic detection of the events, estimating the event energy, and estimating the direction of the primary particle. These goals and their relation to the measurement, instrument, and mission requirements, are outlined in Table 1.

Detailed Science Objectives & Expected Results	*Scientific Measurement Requirements*	*Instrument Functional Requirements*	*Mission Functional Requirements (top level)*
GZK neutrino detection	Achieve 300K thermal noise limit Distinguish EMP from background Observe max. ice volume	Antenna/rcvr T < 80 K > 1GHz spectral range Dual-polarization data 2π antenna array Altitude > 30 km.	T < 250 K ambient EMI avoidance Ground/flight calibration Flight path over ice 30 days total flight time
0.1-100 EeV neutrino spectrum	ΔE/E < 1	High linearity/dynamic range < 50% range resolution	< Few km balloon geolocation Ice topography, temperature
Low-resolution EeV neutrino sky map	15° azimuth 2° elevation	Antenna gain calibration to 1dB 1 ns event timing	Balloon pointing knowledge < 1°

Table 1: Science traceability matrix for ANITA science objectives, data products and science results

2.3. Expected results

The minimum detectable flux at a given energy will depend on the total volume observed by ANITA, the neutrino cross section at the given energy, the intensity distribution of the source, the acceptance solid angle of the detector volume, the rate of background events, and the total time of observations. Since the most accessible models for neutrino fluxes predict an isotropic intensity distribution, we assume this case. The observed volume at any given point along the ANITA flight path will depend on the altitude, depth of ice, and ice transparency.

Typically the observed volume to 0.5 km depth from an altitude of 37 km is ~0.7×10^6 km^3 water ($\rho \sim 0.9$ gm/cm^3 for polar ice). A neutrino of energy 5×10^{18} eV will, on average, produce a 10^{18} eV cascade after accounting for inelasticity. The neutrino cross section has risen to the point where only relatively short (< 300 km) chords through the Earth's crust are still allowed. This effective restriction in upcoming angles for the neutrino produces a corresponding restriction in

event nadir angles as observed at the detector, although somewhat relaxed by refraction through the surface. At $5x10^{18}$ eV only about half of the observed volume is available, that nearer the horizon.

For a given volume element near the surface, the emission solid angle which survives total internal reflection is of order 10-20% of the original 0.36 sr. Accounting for transmission losses through the ice and local surface, and beam efficiency at the detector, the average acceptance solid angle per volume element is reduced to $< 10^{-2}$ sr at this energy. The effective volumetric aperture is thus ~3000 km^3sr (water equivalent) at $E_\nu = 5x10^{18}$ eV. Using an average total neutrino cross section at this energy of $\sigma_\nu = 0.34x10^{-31}$ cm^2 per nucleon, the minimum detectable flux (MDF) in 10 days observing time is MDF = $2x10^{-17}$ cm^2 s^{-1} sr^{-1}. This result assumes no physics background, which is a plausible assumption at these high energies. The range of predicted fluxes for GZK neutrinos above $5x10^{18}$ eV is 0.8-4.0 $x10^{-17}$ cm^2 s^{-1} sr^{-1} indicating that ANITA could begin to detect such fluxes within a single flight.

Using a detailed Monte Carlo simulation which deals more rigorously with the effects of neutrino propagation and interaction, and the geometric effects of refraction and detector response, we find that the flux sensitivity is comparable to the first-order estimate above. The results of this simulation are used to plot the sensitivity levels in Fig.1. In Table 2 we list the event numbers for various neutrino models which provide upper and lower bounds around the selected models shown in Fig.1. These are estimated for 30 and 100 day exposures at 75% efficiency, and the sensitivity of ANITA in these cases is sufficient to constrain all of the proposed models. The concept of ANITA may be extended in several different directions. For example, a spacecraft version of ANITA might utilize a highly elliptical orbit (HEO) to provide high duty cycle observations of the ice from distances of several thousand km. However, this would raise the effective energy threshold by a large factor, placing the detection of GZK neutrinos well out of reach. An alternative might also be a ground-based system of antenna towers. Such a system would have a low energy threshold but would not view an appreciable volume of ice compared to ANITA. A variety of such alternatives have been evaluated according to their ability to detect predicted EeV neutrino fluxes. The conclusion is that ANITA offers a nearly optimal geometry, combining an EeV energy threshold with an enormous detection volume that is unmatched at these energies by any other detector.

Model	*10 days*	*30 days*	*100 days*
GZK neutrinos (min[1])	1	3	10
GZK neutrinos (max[29])	4	12	40
AGN neutrinos (min[29])	6	18	60
AGN neutrinos (max[30])	13	39	130
Topological defects (min[6])	1.5	5	15
Topological defects (max[5])	190	570	1900

Table 2: Predicted event numbers from various neutrino models for different ANITA flight times, with 75% of flight time over deep ice assumed.

3. DETECTION METHOD

The concept of detecting high energy particles through the coherent radio emission from the cascade they produce can be traced back nearly 40 years to Askaryan[14], who argued persuasively for the presence of strong coherent radio emission from these cascades, and even suggested that this property could lead to neutrino detection by an array of antennas that sensed emission from upcoming events within the radio-transparent outer ~10 m of the lunar regolith. Askaryan noted that any large volume of radio-transparent dielectric, such as an ice shelf or a geologic saltbed, could provide the target material for such interactions and radio emission. In fact all of these approaches are now being pursued.[15, 16, 17] Although significant early efforts were successful in detecting radio emission from high energy particle cascades in the Earth's atmosphere[18], surprisingly little work was done on Askaryan's suggestions that solids such as ice and the lunar regolith could be equally important media for detection, until the mid-1980's, when Markov & Zheleznykh[19] revisited these ideas and confirmed the theoretical basis. More recently Zheleznykh[20], Dagkesamansky & Zheleznykh[21], Zas, Halzen, & Stanev[22], and Alvarez-Muniz & Zas[23] have taken up these suggestions again and have confirmed the basic results through more detailed analysis.

3.1. Proof of principle

An important component in developing radio detection techniques for high energy particles is to validate our understanding of the cascade radio emission process in the energy regime where it is expected to become dominant over all other forms of secondary cascade emission (for example, optical Cherenkov radiation). This occurs at cascade energies in the vicinity of 10^{15} eV. Particles of this energy cannot presently be produced in accelerator facilities, but there are alternative ways to test the radio emission mechanisms using lower energy pulsed charge-particle or gamma-ray bunches at a linear accelerator. Two of the investigators on the team (Gorham and Saltzberg) have performed two experiments along these lines, the first at the Argonne Wakefield Accelerator (AWA) in the fall of 1999[24], and more recently at the Stanford Linear Accelerator Center (SLAC) in the summer of 2000[25]. Because of the importance of these measurements with respect to the ANITA effort, we digress here to discuss these in some detail, focusing on the later, more complete, experiment at SLAC.

The cascades used in this experiment were initiated by intense bunches of pulsed gamma-rays. The gamma-rays were produced via bremsstrahlung from the primary electrons in the linac. A large silica sand target and antennas were placed in a gamma-ray beamline in the Final Focus Test Beam facility at SLAC in August 2000. The apparatus was placed 30 m downstream of the bremsstrahlung radiators that produced a high-energy photon beam from 28.5 GeV electrons. The results described here have been published recently in Physical Review Letters [25], to which we refer the reader for more details. Typical beam currents during the experiment were (0.2–1.0)x10^{10} electrons per bunch. The two bremsstrahlung radiators could be used either separately or in tandem, thereby providing 1%, 2.7% or 3.7% of a radiation length. Thus the effective shower energy induced by the photons could be varied from (0.06–1.1)x10^{19} eV per bunch. The size of the photon bunch at the entrance of the silica sand target was less than several mm in all dimensions, and the electrons were directed away from the target and dumped separately to avoid any interference from their induced fields. The target was a 1-m by 1-m by 4-m container built largely from non-conductive materials such as wood and plastic which was filled

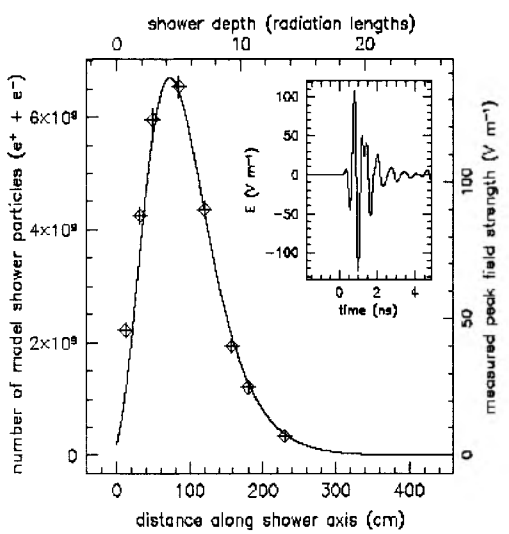

Figure 4: Dependence of pulse filed strength on position along the shower. Inset: typical pulse profile.

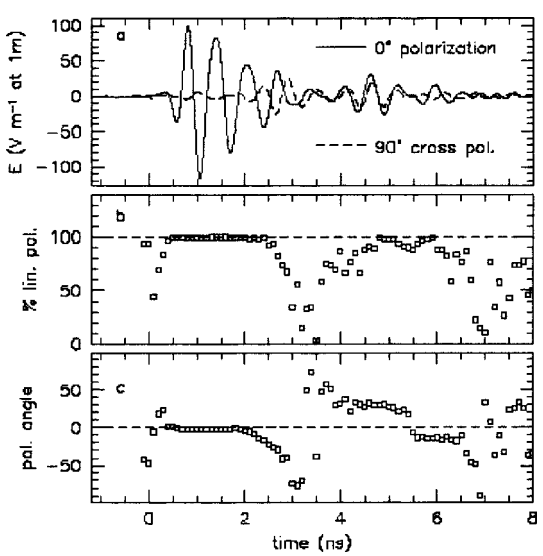

Figure 5: Top: Co- and cross-polarized pulse profiles. Middle: degree of polarization of the pulse. Bottom: Angle of polarization plane of the pulse.

with 3200 kg of dry silica sand. The sand target was rectangular in cross section perpendicular to the beam axis, but the vertical faces on both sides were angled to facilitate transmission of radiation arriving at the Cherenkov angle (about 51° in silica sand at microwave frequencies). Fig. 4 shows a typical pulse profile (inset) and a set of measured peak field strengths for pulses taken at different points along the shower. The plotted curve shows the expected profile of the total

number of particles in the shower, based on the Kamata-Nishimura-Greisen[25] approximation. Here the field strengths have been scaled in the plot to provide an approximate overlay to the relative shower profile. Clearly the pulse strengths are highly correlated to the particle number profile. Since the excess charge is also expected to closely follow the shower profile, this result is consistent with Askaryan's hypothesis. Pulse polarization was measured with an S-band (2 GHz) horn directed at a shower position 0.5 m past the shower maximum. Fig. 5(a) shows the pulse profile for both the 0° and 90° (cross-polarized) orientations of the horn. Fig. 5(b) and (c) show the derived degree of linear polarization and the angle of the plane of polarization, respectively. The results are completely consistent with Cherenkov radiation from a source along the shower axis. Since the position was downstream of shower maximum, late reflections from the upper surface of the sand enter the pulse profile, resulting in a loss of polarization beyond ~2 ns. Fig. 6 (left pane) shows a typical sequence of pulse field strengths versus the total shower energy, which was varied both by changing the beam current and the thickness of the bremsstrahlung radiators. The fitted linear rise of field strength with beam current is consistent with complete coherence of the radiation, implying the characteristic quadratic rise in the corresponding pulse power with shower energy. Fig. 6 (right pane) shows the spectral dependence of the radiation, which is consistent with the linear rise with frequency that is also characteristic of Cherenkov radiation. Also shown is a curve based on a parameterization of Monte Carlo results[22]. The uncertainties are estimates of the combined systematic and statistical uncertainties. Note that the figure compares absolute field strength measurements to the predictions and the agreement is very good. In summary, there is clear experimental evidence that Askaryan's hypothesis is confirmed and that the predicted emission from high-energy cascades is present in the expected amounts. This lends strong support to experiments, including ANITA, designed to exploit this effect for high-energy neutrino and cosmic ray detection.

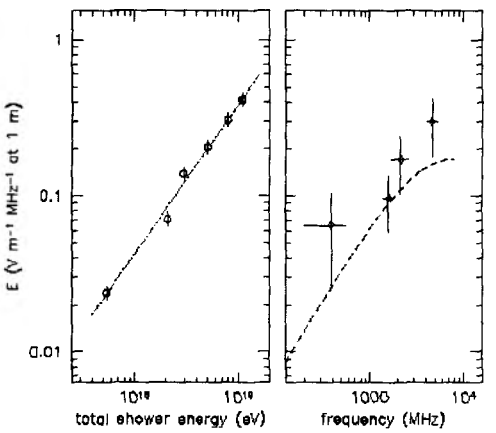

Figure 6: Coherence and absolute power measurements on the Cherenkov radio pulses at SLAC

4. BASELINE DESIGN

The ANITA mission is unusual for astrophysics missions in its reliance on the Antarctic ice as the Cherenkov radiator in an enormous scale of detector. The onboard antenna clusters by analogy play the role of photomultipliers in a Cherenkov or scintillation counter, by collecting the secondary emission from the medium in which the particle of interest interacts. For this reason one of the primary mission constraints is that ANITA spend as much time as possible with a field of view containing only deep ice. Fortunately this constraint is not a major restriction for the mission, since in fact the typical flight path for a circumpolar Antarctic flight spends 100% of its time over the ice. This is shown in Fig. 7. The plot shows the coastal boundary of Antarctic ice, and indicates the average balloon flight path by a circle that crosses McMurdo Station (the launch site). A series of fields-of-view of the balloon are indicated by the smaller circles that are centered along the flight path. These indicate the distance to the horizon which occurs at about 680 km for a 37 km altitude. Approximately 70% of the field of view is of the ice sheet with average depth of order 2 km or more. Another 15% occurs over shallower coastal ice or over the ice shelves, with depths of several hundred meters to 1 km. The balance of the observed field of view is of the Ross and Weddell seas. Typical mission durations for one circumpolar flight are of order 10-12 days. We note that recent Antarctic flights are attempting to execute more than one circumpolar orbit during a mission, and flight durations in the near future are expected to approach 30 days. Our mission plan will be to take advantage of such improvements if possible, but we assume 3 flights of ten days each to achieve our 30 day goal.

4.1. Instrument design overview

The ANITA instrument is fundamentally a broadband antenna cluster, which is arrayed in such a way as to be optimized for pulse detection and characterization while providing nearly a 2π field of view. The signal from each antenna is split into two circular polarizations and four frequency channels and digitized. The digitized signals are stored in a buffer for about 20 microseconds. The digitized signals are also sent to a trigger logic circuit. When the trigger conditions are

satisfied the relevant data from the buffer is extracted and stored. The stored data is then sent back to a ground station at a low rate.

The trigger requirements can be modified but will require that a pulse be seen in 1) several antennas that have overlapping fields of view, 2) most of the frequency channels, 3) both polarizations, and 4) at the same time in all detectors. The trigger is inhibited if the pulse is present in antennas that do not have overlapping fields of view. The trigger mechanism should reduce the signal antenna rate, due to thermal noise, of ~3.5 kHz to a recording rate of about 1 event every few minutes.

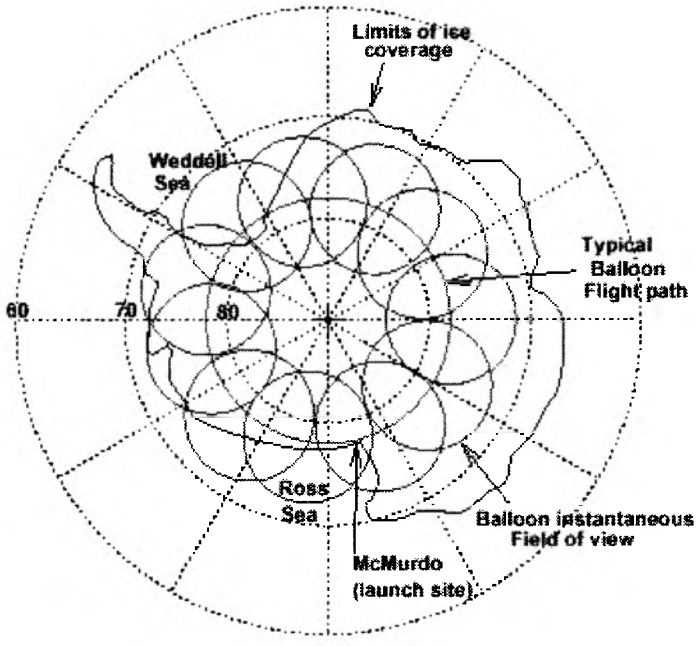

Figure 7: Map of Antarctic ice boundary with balloon flight path and instantaneous fields of view shown.

The data volume at this rate is about 43 Mbytes/day. There will be on board storage greater than 20 Gbytes but the data will also be down linked through the Tracking and Data Relay Satellite System (TDRSS) at rate of 4 kbits/sec. The downlinked data will be forwarded to the National Scientific Balloon Facility in Palestine, Texas. The primary reason for the data downlink is to save the data even if the instrument is lost, but the data will also be monitored during the flight.

An uplink capability to the instrument exists and modifications to the instrument, primarily having to do with triggering, can be made if anomalous conditions are detected.

Figure 8 shows the ANITA payload. The cluster of 16 antennas in each ring provides the azimuthal coverage. From the amplitude ratios of signals in adjacent antennas the azimuthal direction of the pulse can be estimated with an accuracy of about 12°. The two vertically displaced antenna clusters allow determination of the vertical angle of the pulse, with an accuracy of about 2° at the horizon, using the time of arrival of the pulse at the two clusters. The vertical angle is used to compute the range to the event which is the most important geometric parameter is estimating the event energy. At the horizon the fractional range resolution about 50% and improves to 10% near the nadir.

Sun sensors and an anti-rotation bearing are used to stabilize the instrument and keep the solar array pointed at the Sun.

More details concerning the instrument design are presented in a companion paper in this proceedings.

4.2. Background interference

Because ANITA will operate with extremely high radio bandwidth over frequencies that are not reserved for scientific use, the problem of radio backgrounds, both anthropogenic and natural, is crucial to resolve. We have noted above that the thermal noise floor provides the ultimate background limitation, in much the same way that photon noise provides the ultimate limit to optical imaging systems. Here we briefly address backgrounds from other sources.

4.2.1. Lightning and cosmic ray air shower backgrounds

Lightning is known to produce intense bursts of electromagnetic energy, but these have a spectrum that falls steeply with frequency, with very little power extending into the UHF and microwave regimes. Lightning is also unknown on the

Antarctic continent, although it does occur over the Southern Ocean.[26, 27] We do not expect lightning to comprise a significant background to ANITA. Cosmic ray air showers at energies above 0.1 EeV also produce an electromagnetic pulse, known from observations since the late 1960's. Although these pulses may have a weak component associated with the Askaryan effect, the dominant emission comes from synchrotron radiation in the geomagnetic field. Again this radiation falls steeply at frequencies above 100 MHz, and although such events may occasionally trigger a system like ANITA, the spectral characteristics will be unmistakably different from the ice cascade emission.

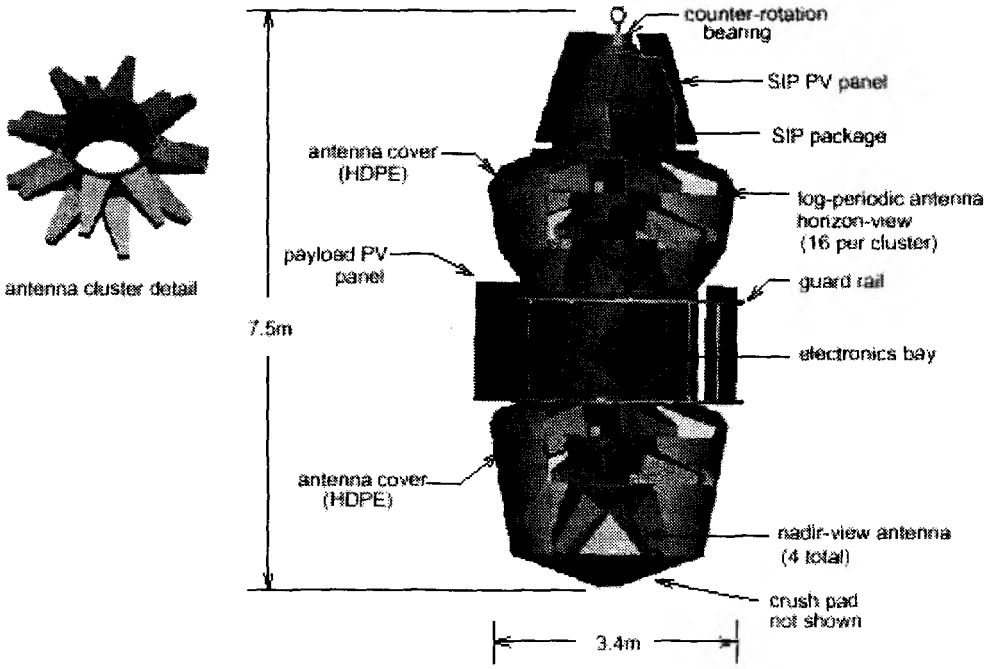

Figure 8: Layout of the ANITA payload showing the antenna geometry. The antenna covers are shown partly cut away for clarity.

4.2.2. Satellite signals

Fortunately for ANITA, satellites transmit power that is generally low in the bands of interest. For example, the GPS constellation satellites at an altitude of 21000 km, have transmit powers of order 50W in the 1227 MHz and 1575 MHz bands, with antenna gains of 11-13 dBi. The implied power at the earth's surface is -160 dBW/m^2 maximum in the 1227 MHz band. The implied field strengths for ANITA are of order 0.2 μV/m. These levels are easily filtered with tunable notch filters for the satellite frequencies of interest. All Earth-orbiting satellites are constrained by the International Telecommunications Union (ITU) to maintain a power level that produces no more than -154 dBW/m^2 at Earth. These power levels are weak enough that they will not saturate ANITA LNAs even if they are not pre-filtered. Since they are narrow-band signals they cannot produce the broadband EMP events to which ANITA will be sensitive. However, an important aspect of the ANITA front end will be a filterbank that removes these and other known narrow-band signals prior to launch. This will reduce the effective system temperature which would otherwise be increased somewhat by the integrated effects of narrow-band carrier signals diluted across the ANITA bandwidth. The number and performance of the filters would be determined during the EMI background survey discussed below.

4.2.3. Terrestrial signals

The primary risk for terrestrial signals is not that they trigger the system, although they will almost certainly do so on occasion. Such triggers are easily recognized in post analysis since they cannot reproduce the characteristics of the cascade pulses. The greater issue for ANITA occurs if there is a strong transmitter in the field of view which saturates the LNA, causing its gain to drop so that the sensitivity in that antenna is lost. Our present LNA design will tolerate up to about 6 dBm output before saturation, with an input stage gain of order 25 dB. Thus a signal of 10 μW coupled into the

antenna would pose a risk of saturation and temporary loss of sensitivity. Since the antenna effective area approaches 1 m^2 at the low end of the band, ANITA could therefore tolerate up to a 1 MW transmitter at or near the horizon, or a 5 kW transmitter near the nadir. Most of the higher power radar and other transmitters in use in Antarctic are primarily at the South Pole and McMurdo stations. The South Pole station is not in ANITA's view during a typical flight, and McMurdo station will only be in view during brief periods during the flight.

4.2.4. EMI background survey

We propose to include, as part of a phased approach to the mission, an early study of the ambient background noise by deploying a limited Antarctic payload either as a piggy-back package on another flight, or as a separate small-payload balloon flight. This survey would be performed as early as is feasible during the project. Prior to obtaining results of this survey mission we would carry several parallel interference mitigation strategies within the design, and the outcome of this early study would then allow a selection of the final configuration. We stress here that we do not anticipate that the results of this study could provide information that would make the mission unfeasible; rather we expect that more precise knowledge of the nature of the backgrounds will reduce risk in the later phases of the mission, and will also allow us to exercise both the TDRSS telemetry package and provide valuable experience to the team which will help to ensure success in the main launch.

Since the development of a complete balloon payload and gondola for this effort would add significantly to the cost and schedule, we have identified an existing payload and gondola which can be readily adapted for our purposes, the Balloon Air Cherenkov payload (BACH). This package was developed by Bartol for cosmic ray composition studies and flown from Palestine in 1998. The mission was not selected for further long-duration flights and the payload is now available. The heart of the system provides a crucial piece of hardware necessary for our background study: a high bandwidth digital oscilloscope, interfaced to a line-of-sight telemetry system, and including onboard storage for the digitized data samples. The BACH system originally recorded photomultiplier pulses from atmospheric cosmic ray events [28]. We will replace the photomultipliers with commercial antennas and off-the-shelf RF conditioning hardware. There is sufficient lead time planned to allow us to adapt our mitigation strategies to the actual measured environment as part of the final integration and testing.

5. SUMMARY

ANITA is a long-duration balloon mission the will address the question of the origin of the highest energy cosmic rays. ANITA will break completely new ground by detecting neutrinos associated with ultra-high energy cosmic ray interactions throughout the universe. The high energy neutrinos are detectable through their interactions within the Antarctic ice sheet, which ANITA will utilize as a detector target which effectively converts the neutrino interactions to radio pulses.

ANITA will monitor more than 1 million cubic kilometers of the Antarctic ice sheet from a 40 kilometer balloon altitude. An onboard antenna array will be sensitive to the electromagnetic pulse (EMP) that is produced when the neutrino interaction initiates a cascade of relativistic particles in the ice. The generation of such EMP events has been confirmed by accelerator experiments. These events provide a powerful new technique in the search for neutrinos and open a potentially new window on previously unseen forms of energy in the universe. ANITA will act as a pathfinding mission of unequaled sensitivity in the new filed of neutrino astronomy.

6. ACKNOWLEDGEMENTS

We would like to thanks the staff at JPL for their support during the preliminary design phase of ANITA; notably Conrad Foster, Aaron Bachelder, Bill Imbriale, Dave Fort, Elliott Sigman, and Steve Lowe. This work was supported in part by NASA through JPL and by the US Department of Energy.

7. REFERENCES

1. R. Engel, D. Seckel, & T. Stanev, "Neutrinos from propagation of ultra-high energy protons," 2001, Bartol Research Institute Report Number BA-01-01 (astro-ph/0101216) and references therein provides a recent comprehensive summary of the GZK neutrino connection.
2. K. Greisen, "End to the Cosmic Ray Spectrum?," *Phys. Rev Lett.* **16**,748 (1966).
3. G.T. Zatsepin and V. A. Kuz'min, *JETP Letters* **4**, 78 (1966).
4. A. Muecke, R.J. Protheroe, *Astropart. Phys.* **15**, 121 (2001).
5. S. Yoshida, G. Sigl, S. Lee, *Phys. Rev. Lett.* **81**, 5505 (1998).
6. G. Sigl, *Nucl. Phys. Proc. Suppl.* 87, 439-441 (2000).
7. D. J. Bird *et al.*,"Evidence for Correlated Changes in the Spectrum and Composition of Cosmic Rays at Extremely High Energies,"*Phys. Rev. Lett.* **71**, 3401 (1993); H.Hayashida *et al.*, *Ap. J.* **522**, 225 (1999); C.C. H. Jui *et al.*, *26th International CosmicRay Conference Invited, Rapporteur, and Highlight papers* (AIP Conf. Proc **516**), 370 (2000).
8. T Stanev, et al.,"The Arrival directions of the most energetic cosmic rays," *Phys. Rev. Lett.* **75**, 3056 (1995); N.Hayashida et al., "Possible Clustering of the Most Energetic Cosmic Rays Within a limited Space Angle Observed by the Akeno Giant Air Shower Array," *Phys. Rev. Lett.* 77, 1000 (1996).
9. A. Kusenko & M. Postma, "Neutrinos produced by ultrahigh-energy photons at high red shift," *Phys. Rev. Lett.* **86**, 1430, (2001); G. Gelmini, & A. Kusenko, "Unstable super-heavy relic particles as a source of neutrinos responsible for the ultrahigh-energy cosmic rays," *Phys. Rev. Lett.* **84**, 1378 (2000).
10. C.T. Hill and D, N. Schramm, "Ultrahigh-energy cosmic-ray spectrum," *Phys. Rev.D* **31**,564 (1985); F.W. Stecker, "Effect of Photomeson Production by the Universal Radiation Field on High-Energy Cosmic Rays," *Phys. Rev. Lett.* **21**, 1016-1018 (1968).
11. see AGASA contributions to 27th ICRC, Hamburg 2001 (in press 2001); M. Takeda, *et. al.*, *Phys. Rev. Lett.* **81**, 1163 (1998); N. Hayashida, *et. al.*, *Astropart.Phys.* **10**, 303 (1999); N. Hayashida, *et. al.*, *Astrophys. J.* **522**, 225 (1999).
12. T.Abu-Zayyad, *at. al.*, "Measurement of Cosmic Ray Energy Spectrum and Composition from 10^{17} to $10^{18.3}$ eV Using a Hybrid Fluorescence Technique", *Astrophys. J.* **557**, 686 (2001).
13. J. G. Learned, & K. Mannheim, "High Energy Neutrino Astrophysics," *Ann Rev. Nucl.Part. Sci.* **50**, 679-749, (2000) is an excellent recent review on this topic.
14. G. A. Askaryan, *JETP* **14**, 441 (1962); also *JETP* **21**, 658 (1965).
15. P. W. Gorham, K. M. Liewer, C. J. Naudet, D. P. Saltzberg, and D. Williams, "Radio limits on an isotropic flux of >100 EeV cosmic neutrinos," *Proc. RADHEP 2000*, ed. D. Saltzberg & P. Gorham, (Amer. Inst. Phys. press), in press, (2001); astro-ph/0102435.
16. D. Seckel, "In ice radio detection of GZK neutrinos", *RADHEP-2000*; astro-ph/0103300.
17. Peter Gorham, David Saltzberg, Allen Odian, Dawn Williams, David Besson, George Frichter, Sami Tantawi, "Measurements of the Suitability of Large Rock Salt Formations for Radio Detection of High Energy Neutrinos", to be submitted to Nucl. Inst. and Meth.; hep-ex/0108027.
18. J. V. Jelley *et al.*, *Nature* **205**, 327 (1965); *Nuovo Cimento* **A46**, 649 (1966); N. A. Porter *et al.*, *Phys. Lett.* **19**, 415 (1965); S.N. Vernov *et al.*, *Pis'ma v ZhETF* **5**, 157 (1967) [*Sov. Phys.–JETP Letters* **5**, 126 (1967)]; *Can. J. Phys.* **46**, S241 (1968); P.R. Barker, W. E. Hazen, and A. Z. Hendel, *Phys. Rev. Lett.* **18**, 51 (1967); W. E. Hazen, *et al.*, *ibid.* **22**, 35 (1969); **24**, 476 (1970); D. Fegan & N. A. Porter, *Nature*, 1968; H.R. Allan, in *Progress in Elementary Particles and Cosmic Ray Physics*, v. 10, edited by J. G. Wilson and S. G. Wouthuysen (North-Holland, Amsterdam, 1971), p. 171, and references therein.
19. M. Markov & I. Zheleznykh,"Large scale Cherenkov detectors in ocean, atmosphere and ice," *Nucl. Instr. Meth. A* **248**, 242 (1986).
20. I. M. Zheleznykh, *1988 Proc. Neutrino '88, World Scientific*, Boston, ed. J. Schreps. 528.
21. R. D. Dagkesamansky, & I. M. Zheleznykh, *JETP Lett.* **50**, 233 (1989).
22. E. Zas, F. Halzen, and T. Stanev, *Phys. Rev. D* **45**, 362 (1992).
23. J. Alvarez-Muniz & E. Zas, "Prospects forradio detection of extremely high energy cosmic rays and neutrinos in the Moon," *Proc. RADHEP 2000*, ed. D. Saltzberg & P.Gorham, (Amer. Inst. Phys. press), in press, (2001); astro-ph/0102173.

24. P. W. Gorham, D. P. Saltzberg, P. Schoessow, et al., "Radio-frequency measurements of coherent transition and Cherenkov radia-tion: Implications for high-energy neutrino detection," *Phys. Rev. E* **62**, 8590, (2000); hep-ex/0004007.
25. D. Saltzberg, P. Gorham, D. Walz, et al., "Observation of the Askaryan Effect: Coherent Microwave Cherenkov Emission from Charge Asymmetry in High Energy Particle Cascades," *Phys. Rev. Lett.* **86**, 2802 (2001); hep-ex/0011001.
26. A.R. Jacobson, pers. communication, (2001).
27. A. R. Jacobson, K. L. Cummins, M. Carter, et al., "FORTE radio-frequency observations of lightning strokes detected by the National Lightning Detection Network," *JGR bf 105*, **15**, 653 (2000); R. Roussel-Dupre', & A.V. Gurevich, "On runaway breakdown and upward propagating discharges," *JGR* **101**, 2297 (1996); A. V. Gurevich, K. P. Zybin, and R. Roussel-Dupre', "Lightning Initiation by simultaneous effect of runaway breakdown and cosmic ray showers," submitted to *JGR* (2001).
28. J. Clem, W. Droege, P.A. Evenson, H. Fischer, G. Green, D. Huber, H. Kunow, and D. Seckel, "A Measurement of the Flux of Cosmic Ray Iron at $5x10^{13}$ eV," *Astroparticle Phys.* **16**, pp387-395, 2002.
29. R. J. Protheroe, & T. Stanev, *Phys. Rev. Lett.* **77**,3708.
30. K. Mannheim, R.J. Protheroe, J.P. Rachen *Phys. Rev. D* **63** (2001) 023003.